Power Deposited on a Dielectric by Multipactor

Lay-Kee Ang, Y. Y. Lau, Rami A. Kishek, and Ronald M. Gilgenbach, *Senior Member, IEEE*

***Abstract*—We use a simple transmission line model to evaluate the rf power deposited on a dielectric window by multipactor discharge. The calculation employs Monte Carlo simulation, using realistic secondary electron yield curves as input, and taking into account the distributions in the emission velocities and emission angles of the secondary electrons. Beam loading on the external rf, as well as the evolution of the dc electric field due to dielectric charging, are also accounted for. It is found that the buildup of the multipactor space charge, rather than beam loading, causes saturation. Over a wide range of operating conditions and materials, it is found quite generally that the multipactor delivers on the order of 1 percent, or less, of the rf power to the dielectric. A simple estimate is given in support of this ratio, using the susceptibility diagram that was constructed from kinematic considerations. Comparison with experimental results is given.**

I. Introduction

MULTIPACTOR discharge is an ubiquitous phenomenon observed in a multitude of devices that employ microwaves [1]. It may occur when a metallic gap or a dielectric surface is exposed to an ac electric field under some favorable conditions, and its avoidance has been a major concern among workers on high power microwave sources, rf accelerators, and space-based communication systems [1]–[7]. While there is a sizable literature on the subject scattered here and there throughout the years, (most of which are in the form of unpublished memo reports or conference proceedings [4], [7]), only a few in particular have been devoted to theoretical study of multipactor on a dielectric, such as an rf window [2], [4], [8].

Failure of rf windows remains not fully understood. In his 1988 thesis entitled, "High Power Microwave Window Failure," Rimmer [4, p. 111] found that the dielectric (ohmic) loss in the window is unable to cause thermal or stress failure. He went on to say that "the most important factor in the failure mechanism as yet uncharacterized is the contribution from multipactor in the cavity or on the window" and that "it does seem likely that multipactor could supply sufficient heat by direct absorption from the rf field to provide the necessary input to cause failure" [4, p. 107]. In this paper, we use a simple model to analyze the temporal evolution of the single-surface multipactor on a dielectric, paying special attention to the saturation mechanism, saturation level, the loading of the external rf by the presence of multipactor, and the evolution of the dc electric field that results from dielectric charging.

Manuscript received September 23, 1997; revised January 14, 1998. This paper was presented in part at the International Workshop on High Power Microwave Generation and Pulse Shortening, Edinburgh, U.K., June 1997. This work was supported by the Multidisciplinary University Research Initiative (MURI), managed by the Air Force Office of Scientific Research and subcontracted through Texas Tech University, by the Department of Navy Grant N00014-97-1-G001 issued by the Naval Research Laboratory, and by the Northrop Grumman Industrial Associates Program.

L.-K. Ang, Y. Y. Lau, and R. M. Gilgenbach are with the Department of Nuclear Engineering and Radiological Sciences, University of Michigan, Ann Arbor, MI 48109-2104 USA (e-mail: yylau@engin.umich.edu).

R. A. Kishek was with the Department of Nuclear Engineering and Radiological Sciences, University of Michigan, Ann Arbor, MI 48109-2104 USA. He is now with the Institute for Plasma Research, University of Maryland, College Park, MD 20742 USA.

Publisher Item Identifier S 0093-3813(98)04278-7.

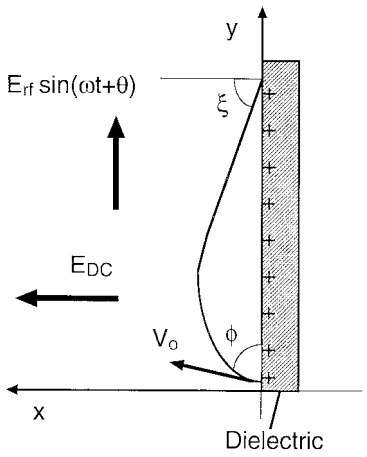

Fig. 1. Schematic of a single-surface multipactor in a parallel rf and normal dc electric fields.

Recently, we initiated a theoretical study of multipactor discharge on dielectric [8]. We used Monte Carlo simulation to obtain the range of rf electric field over which multipactor can occur. The result is applicable to a wide range of materials, and over a wide range of frequencies. We used realistic secondary yield curves as input to the Monte Carlo simulation, which assumed a distribution of velocity and of emission angle for the secondary electrons. These simulations assumed a constant amplitude rf electric field $(E_{\rm rf})$ parallel to the dielectric surface and a constant dc electric field $(E_{\rm DC})$ normal to the dielectric surface (Fig. 1). By examining the multipactor growth (and suppression) for various combinations of these fields, the susceptibility diagram in the $(E_{\rm rf}, E_{\rm DC})$ plane was constructed, over a wide range of frequencies and dielectric materials [8]. This kinematic study ignored all beam loading effects on the external rf and space charge effects as the multipactor grew.

In the present paper, we extend our Monte Carlo simulation and introduce two novel aspects. We account for the loading of rf by the multipactor discharge. The reflection of the incident electromagnetic wave onto the dielectric, by the multipactor, is computed using a transmission line model. Secondly, we include self-consistently the evolution of the charging field, $E_{\rm DC}$, that is normal to the surface [9]. We assume that this charging field is caused by the positive charges that are spread uniformly over the dielectric surface (Fig. 1). For most

of the simulations, the total positive charge is assumed to be equal (but opposite in sign) to the instantaneous charge residing in the multipactor electrons. It turns out that it is this space charge effect that leads to the saturation of multipactor discharge. Beam loading is relatively unimportant to the saturation mechanism, unlike the situation in a cavity [7]. At saturation, the multipactor typically consumes about 0.5 per cent of the rf power of the incident electromagnetic wave, to within factors of 2, over a wide range of operating conditions. The time required for saturation is relatively rapid. The bounce time of a typical multipactor electron at saturation is much less than the rf period. The saturation levels may be qualitatively determined from the susceptibility diagram that was derived from kinematic considerations [8]. We will show that our theories may account for several interesting features of Rimmer's experiments, supporting his speculations quoted above.

II. The Model

The mechanism of the single-surface multipactor on a dielectric is shown in Fig. 1. A secondary electron is emitted from the dielectric surface with a random velocity, v_o, and a random angle, ϕ, with respect to the positive y-axis. It is subjected to an rf electric field and the dc charging electric field [9]. The rf electric field, of magnitude $E_{\rm rf}$ and frequency ω, acts only in the y-direction and imparts energy to the multipactor electron, as well as translates it along the y-axis. The dc electric field, E_{DC}, does not impart any energy to the electron. This electron, emitted from the surface with a nonzero emission velocity, is bent back by the restoring dc electric field and strikes the surface at a later time. During its transit, the electron gains energy only from the rf electric field, in a direction parallel to the surface. Thus upon impact, the electron strikes with much larger energy, at the same time emitting a number of secondary electrons by the process of secondary electron emission [10], [11]. These secondaries also leave the surface and strike back at a later time, in the process gaining energy from the rf that is eventually deposited onto the dielectric surface. It is this energy deposition that we shall analyze in this paper.

A. The Circuit Model

To analyze the amount of power delivered by multipactor onto the dielectric window, we shall use a one-dimensional (1-D) model. Consider a plane electromagnetic wave incident onto the dielectric window [Fig. 2(a)]. In the absence of multipactor, this plane wave is assumed to be perfectly transmitted through the dielectric window with zero reflection. Such an incident plane wave may then be represented as a rightward traveling voltage pulse V_+ on a transmission line, of characteristic impedance Z_o, and terminated by a matched load of impedance Z_o [Fig. 2(b)]. The presence of multipactor will induce partial reflection and partial absorption of the incident wave, the remainder being transmitted. All of these can be simply modeled by a variable impedance, through which the multipactor current $I_m(t)$ flows [Fig. 2(b)]. A nonzero I_m gives rise to reflection, and the amount of power absorbed

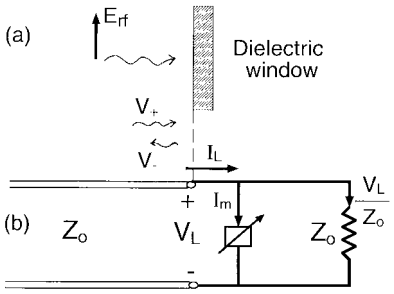

Fig. 2. Transmission line analog of an incident electromagnetic wave onto a dielectric window.

by the multipactor is simply $V_L I_m$, where V_L is the voltage across the load.

Let V_+ be the incoming wave, and V_- be the reflected wave at the load. Continuity of voltage and current at the load gives [Fig. 2(b)]

$$V_+ + V_- = V_L, \tag{1}$$

$$\frac{V_+}{Z_0} - \frac{V_-}{Z_0} = I_L = I_m + \frac{V_L}{Z_0}. \tag{2}$$

Equations (1) and (2) may be combined to yield the reflected wave V_- in terms of the multipactor current

$$V_- = -\tfrac{1}{2} Z_0 I_m. \tag{3}$$

To calculate the multipactor current I_m, we equate the instantaneous power consumed by multipactor, P_m, to the work done on the multipactor electrons by the tangential rf field on the dielectric surface

$$P_m = V_L I_m = -\frac{eN}{\tau} \int_t^{t+\tau} dt'\, E_{\rm rf}(t') v_y(t'). \tag{4}$$

In (4), N is the total number of multipactoring electrons at time t, τ is the time of flight of the multipactor electrons at time $t, E_{\rm rf}$ is the total rf electric field on the surface, and v_y is the y-component velocity of the multipactor electrons (Fig. 1). All quantities pertaining to electrons, such as N and τ, are to be obtained from the Monte-Carlo simulations. The rf electric field in the integral of (4) is a combination of the incident and reflected waves. Even though the latter turns out to be small, it is kept in the simulations. Equations (1), (2), and (4) are the governing equations for V_-, V_L, and I_m. The conversion between the rf electric field $E_{\rm rf}$ and the transmission line voltage V is through $V = E_{\rm rf} A^{1/2}$ where A is the surface area in the 1-D model.

B. Electron Dynamics

The multipactor electrons are acted on by the instantaneous rf electric field, $E_{\rm rf} \sin(\omega t + \theta)$, and by the instananeous charging electric field $E_{\rm DC}$, both being treated as constant over a transit time [9]. Referring to Fig. 1, we obtain from the force law

$$v_x = -\frac{e}{m} E_{\rm DC} t + v_o \sin\phi \tag{5}$$

$$v_y = \frac{e}{m\omega} E_{\rm rf} [\cos(\omega t + \theta) - \cos\theta] + v_o \cos\phi \tag{6}$$

where the last terms account for the emission velocity at $t = 0$. From (5), it is clear that the transit time τ is given by

$$\tau = 2mv_o \sin\phi / eE_{\rm DC}. \tag{7}$$

The dc electric field is allowed to evolve. It has two components, the constant part $(E_{\rm DC0})$ that is assumed to have existed prior to the multipactor discharge, and the time-varying part $(E_{\rm DC1})$ that is caused by the positive charge left on the dielectric surface as a result of the ejection of the multipactor electrons by secondary emission. Lacking a reliable means to calculate $E_{\rm DC1}$, we simply assume that the positive charge left behind on the dielectric surface is uniformly distributed. Thus, $E_{\rm DC1} = \sigma/2\varepsilon_o = eN/2A\varepsilon_o$ where σ is the surface charge density, N is the total number of multipactor electrons in flight, A is the surface area of the dielectric, and ε_o is the free space permittivity. Thus, the instantaneous dc electric field is

$$E_{\rm DC} = E_{\rm DC0} + \frac{eN}{2A\varepsilon_0} \tag{8}$$

which evolves as the multipactor charge eN builds up. The initial charging field, $E_{\rm DC0}$, will be chosen to ensure initial growth of multipactor (see below).

Upon using (6)–(8) in the right hand side of (4), we obtain the power consumed by multipactor, averaged over each bounce, in terms of N and τ, quantities associated with each bounce.

C. Electron Emission Model and Monte Carlo Simulations

Upon impact on the surface, a primary electron produces an average number of secondary electrons, called the secondary electron yield, δ. This yield depends on the material, and is a function of the impact energy of the primary electron, E_i, and the angle to the normal, ξ, at which it strikes the surface [10]–[12]. For the dependence of yield on impact energy, we will adopt Vaughan's empirical formula [12], for normal incidence,

$$\delta = \delta(E_i) \cong \delta_{\max}\left(we^{1-w}\right)^k \tag{9}$$

where $\delta_{\max}$ is the maximum value of $\delta, w = E_i/E_{\max}, E_{\max}$ being the impact energy which yields $\delta_{\max}$, and $k = 0.62$ for $w < 1$ and $k = 0.25$ for $w > 1$. Two values of impact energy, termed the first and second crossover points, E_1 and E_2, respectively, result in a yield of 1, while $\delta > 1$ in between. By setting the right hand side of (9) equal to unity, we obtain $E_1/E_{\max}$ and $E_2/E_{\max}$ as a function of $\delta_{\max}$ (Fig. 3). For impact at an angle, the parameters $E_{\max}$ and $\delta_{\max}$ are adjusted in calculating the yield, according to the following equations [12]:

$$E_{\max} = E_{\max 0}\left(1 + \frac{k_s\xi^2}{\pi}\right)$$
$$\delta_{\max} = \delta_{\max 0}\left(1 + \frac{k_s\xi^2}{2\pi}\right). \tag{10}$$

Here $E_{\max 0}$ and $\delta_{\max 0}$ are the parameters for an impact angle of 0 (i.e., normal to the surface), and k_s is a surface smoothness factor ranging from 0 for a rough surface to 2 for a polished surface. In this paper we set $k_s = 1$, representing a typical dull surface [12]. It is worth noting that in this situation, since the electrons gain their energy from the parallel rf, most impacts will be at almost grazing incidence (i.e., $\xi \leq \pi/2$).

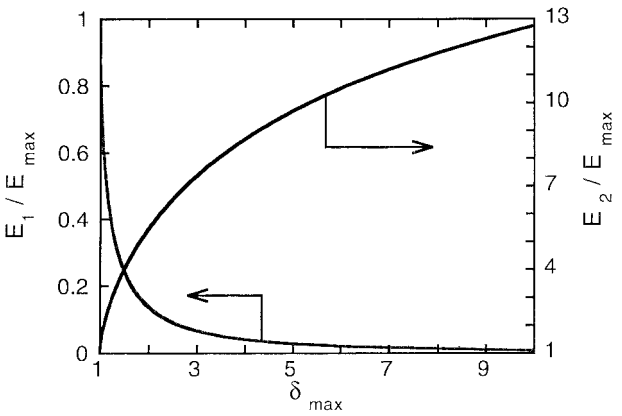

Fig. 3. The first and second crossover energy $E_{1,2}$ as a function of $\delta_{\max}$, according to Vaughan's empirical formula for secondary yield.

To calculate the evolution of the multipactor discharge, we follow the trajectory of a weighted macroparticle over a large number of impacts in a Monte Carlo simulation [8]. The initial rf phase, θ, is uniformly distributed over $0 < \theta < 2\pi$. Each time a macroparticle leaves the surface, we assign it a random initial energy $E_o = \frac{1}{2}mv_o^2$ and angle ϕ, according to the following distributions:

$$f(E_o) = \frac{E_o}{E_{om}^2} e^{-(E_o/E_{om})} \tag{11}$$

$$g(\phi) = \frac{1}{2}\sin\phi \tag{12}$$

where E_{om} is the peak of the distribution of emission energies, on the order of the work function, i.e., a few eV [1], [10], [11]. Note that the expected value of E_o is $2E_{om}$, and that $\int g(\phi)\, d\phi = 1$ over $0 < \phi < \pi$. Substituting the random values of initial energy (velocity) and angle into (5) and (6), we obtain the impact energy and, hence, the secondary electron yield from (9) for that transit. We use this value of the yield to adjust the charge on the macroparticle, then emit it again with a random velocity. Equations (5) and (6) are then updated with a new value of $E_{\rm DC}$, [due to the change in the number of multipactor electrons, N; see (8)], and a new value of $E_{\rm rf}$ (due to the absorption of rf power by the multipactor).

Finally, the input parameters that need to be supplied are: the initial rf electric field $E_{{\rm rf}o}$, the initial dc electric field $E_{{\rm DC}o}$, the secondary emission parameters $\delta_{\max o}$ and $E_{\max o}$, the initial energy of emission E_{om}, and the frequency ω. For the present plane wave model, we set the area A to be 10 cm^2, and the characteristic impedance Z_o to be 377 Ω. Transmission through a waveguide can similarly be modeled with an appropriate modification of Z_o.

III. Simulation Results and Interpretation

Before we present the simulation results, let us first discuss the scenarios of the evolution of $E_{\rm rf}$ and $E_{\rm DC}$. From

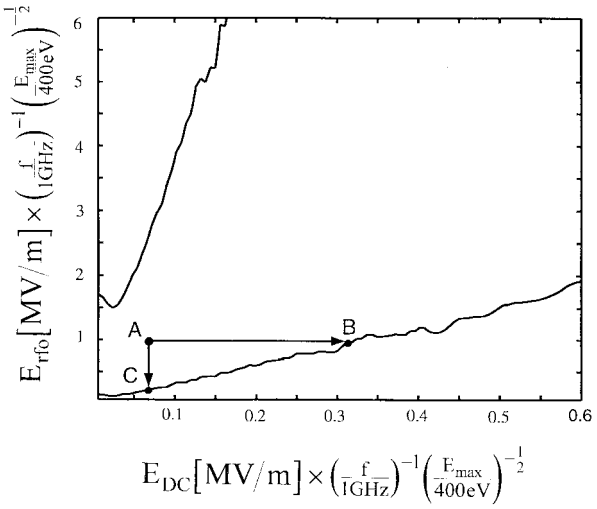

Fig. 4. Multipactor region boundaries in the plane of $(E_{\rm DC}, E_{{\rm rf}o})$ for $\delta_{\max 0} = 3.0, E_{om}/E_{\max 0} = 0.005$. Point A designates an initial combination of electric fields that permit multipactor growth. At saturation, Point B is reached.

our previous kinematic study, we obtain the domain in the $(E_{\rm rf}, E_{\rm DC})$ plane in which multipactor would occur [8]. One such domain is shown in Fig. 4, obtained from the Monte-Carlo simulation with $\delta_{\max o} = 3$, and $E_{om}/E_{\max o} = 0.005$. For values of $E_{\rm rf}$ and $E_{\rm DC}$ outside the two curves in Fig. 4, there would be no multipactor growth, and multipactor growth is possible within these curves. These two curves may be understood as follows [8]: At a fixed value of $E_{\rm DC}$, the rf electric field $E_{\rm rf}$ must lie within a certain range so that the average electron impact energy lies within the two crossover energies, E_1 and E_2, for the average secondary yield to exceed unity (i.e., for multipactor growth). This explains the upper and lower bounds of $E_{\rm rf}$ in Fig. 4. As the dc field is increased, the electrons spend less time in flight [cf., (7)], and so the rf field must increase to maintain the same impact energy and secondary yield. Since the curves in Fig. 4 were obtained for constant $E_{\rm DC}$ and $E_{\rm rf}$, both beam loading and the effects of the multipactor space charge effects were ignored. As we shall see, these curves, obtained from kinematic considerations, turn out to be quite useful even in predicting the rf power delivered to the dielectric by multipactor.

Suppose that the initial values of $E_{{\rm rf}o}$ and $E_{{\rm DC}o}$ lie at Point A of Fig. 4. These initial values lead to multipactor growth, at least initially. Two extreme cases can be envisioned in the subsequent evolution of $E_{\rm rf}$ and $E_{\rm DC}$. First, $E_{\rm DC}$ remains unchanged while $E_{\rm rf}$ drops to Point C because of the absorption of rf power by the growing multipactor. At Point C, the multipactor reaches saturation (in a statistical sense). The other extreme case is that Point A moves horizontally to Point B in Fig. 4. This happens when the multipactor space charge grows so rapidly that $E_{\rm DC}$ increases to the boundary point (B) without sufficiently loading the incident rf. This argument suggests that there will always be saturation of multipactor discharge, and that the saturation point must lie on the lower boundary between Points B and C. It turns out that multipactor saturates much closer to Point B than Point C. That is, *only a small fraction of the incident rf power is absorbed by the multipactor, regardless of the initial conditions and the material properties*. Our analytic estimate, to be given below, corroborates these simulation results.

Let us now consider the most dangerous type of multipactor discharge, for a given initial value of $E_{{\rm rf}o}$. First, if the initial dc electric field, $E_{{\rm DC}o}$, is very high, the initial Point, A, would be very close to Point B. To move from such a Point A to Point B for saturation, the number N of the multipactor electrons need only to grow to a very low value [cf., (8)]. For low values of N, the power consumed by the discharge is low, as clearly seen from (4). Thus, the multipactor that delivers the most power onto the dielectric is one with a very low value of $E_{{\rm DC}o}$. Thus in the simulations, we effectively set the initial dc electric field to the lowest value, barely enough to initiate multipactor growth. In the simulations given below, we set $E_{{\rm DC}o} = 10$ V/m.

We present the simulation results (Fig. 5) with the input data:

$$\begin{aligned} &\delta_{\max o} = 3, E_{\max o} = 420 \text{ eV}, \quad E_{om} = 2.1 \text{ eV} \\ &E_{{\rm rf}o} = 3 \text{ MV/m}, \quad A = 10 \text{ cm}^2, \quad \omega/2\pi = 2.45 \text{ GHz} \\ &E_{\rm DCo} = 10 \text{ V/m}, Z_o = 377\ \Omega. \end{aligned} \tag{13}$$

Fig. 5(a) shows the evolution of the number of multipactor electrons. This number grows exponentially until it reaches a steady state (in the mean). The dashed curves were obtained from the analytic estimates given below. At saturation, the secondary yield has a mean value of unity [Fig. 5(b)]. The fraction of rf power delivered to the dielectric is of order 1 per cent, or less [Fig. 5(c)], a fact observed for simulations using other materials and frequencies, and explained below. This small absorption means that the amount of loading by multipactor is small, leaving the rf electric field amplitude at the surface almost a constant, as shown in the top trace in Fig. 5(d). The charging field, $E_{\rm DC}$, grows to a large value at saturation, as shown in the bottom trace of Fig. 5(d). This suggests the route to saturation from Point A to Point B in Fig. 4. In fact, at saturation at Point B, the impact energy is hovering around the first crossover energy, E_1, in the secondary yield curve. Physically, as the number, N, of multipactor electrons builds up, $E_{\rm DC}$ grows, and the transit time τ decreases. Thus, the energy absorbed from rf, per electron, decreases, and the average impact energy decreases to the first crossover energy E_1 when the steady state is reached. This is also borne out of the simulation data [Fig. 5(e)]. In Fig. 5(f), we see that the transit time between impacts of a multipactor electron becomes much smaller than the rf period at saturation. This fact, $\omega\tau \gg 1$, was actually used [8] to analytically derive the shape of the susceptability boundaries shown in Fig. 4. All of the above features are shared by other runs which use very different parameters from (13).

Let us now explain the various saturation levels based on some simple arguments, using only Fig. 4 and the input data given in (13). For the parameters given in (13), Point B of Fig. 4 gives the saturation dc electric field $E_{\rm DC} = 0.8$ MV/m. This value of $E_{\rm DC}$ yields $N = 8.8 \times 10^{10}$ upon using (8).

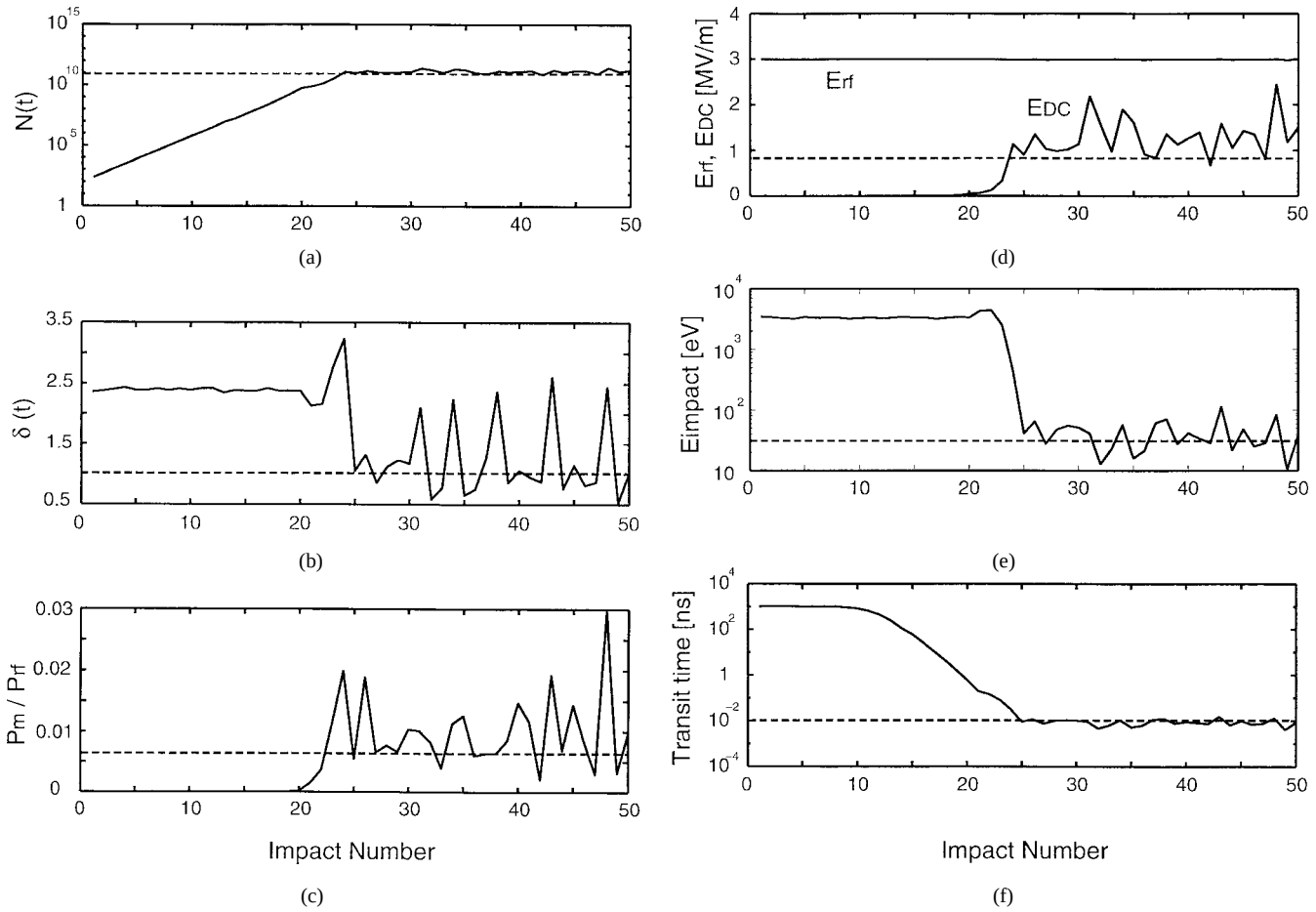

Fig. 5. Evolution of multipactor discharge. The dotted lines represents order-of-magnitude estimates from analytic theory.

Equation (7) then gives the transit time $\tau = 1.2 \times 10^{-11}$ s after we arbitrarily assign the initial normal velocity $(v_o \sin\phi)$ to be equal to $(2E_{om}/m)^{1/2}$. We estimate the fraction of rf power consumed by the multipactor by using (6) into (4). At saturation, $\omega\tau \ll 1$, we then obtain, upon averaging over an rf period

$$\frac{P_m}{P_{\rm rf}} = \frac{e^2 N \tau Z_o}{2\ \text{mA}} = \left(\frac{eE_{\rm DC}}{m}\right)\frac{\tau}{c} \approx 0.004\sqrt{\frac{E_{om}}{1\ \text{eV}}} \qquad (14)$$

where $c = 1/\varepsilon_o Z_o$ is the speed of light. In writing the last expression of (14), we have used (7). The estimate given in (14) is remarkable. It says that the fraction of rf power consumed by multipactor is on the order of a fraction of one per cent of the external rf power, regardless of the frequency, material properties, and rf power (as long as it lies within the susceptibility region shown in Fig. 4). Using (14), that fraction is 0.57%, which is shown in Fig. 5(c). Alternatively, at Point B of Fig. 4, the average impact energy is of order E_1, the first crossover energy of the secondary yield curve. Fig. 3 gives $E_1 = 30$ eV. Thus the average power deposited onto the dielectric by multipactor is of the order $P_m = NeE_1/\tau = 35$ kW. The external rf power is $P_{\rm rf} = 12$ MW, so that $P_m/P_{\rm rf} = 0.0029$, which differs from the above estimate by a factor of two. Such discrepencies are not entirely surprising for these rough estimates (see [8, ref. 15]).

IV. Remarks

From the above analysis of a much simplified model, we draw the following conclusions on multipactor discharge on dielectric.

1) Multipactor typically delivers on the order of one percent or less of the rf power onto the dielectric.
2) As a result, the rf electric field does not suffer much from beam loading. This is in sharp contrast to 2-surface multipactor on metal surfaces [7], [13]–[15].
3) The saturation is caused by the buildup of the surface charge. Thus, the rf and dc fields evolve from Point A to Point B in the susceptibility diagram, Fig. 4.
4) At saturation, the charging field is so strong, and the time of flight of the electrons is so short that the energy gained from the rf field at impact hovers around the first crossover energy E_1 in the secondary yield curve (i.e., Point B in Fig. 4).
5) There is no multipactor growth when the initial fields lie outside the susceptibilty region.

A natural question is whether the relatively small fraction of rf power (<1%) delivered onto the dielectric by multipactor can explain at least some aspects of window failure. Let us once more refer to Rimmer's thesis [4]. His windows transmit 40 kW rf power at 500 MHz through a waveguide. Two windows were tested: (a) the "original window" with an rf

electric field of 400 kV/m and a dielectric loss of 250 W and (b) the "raised window" with an rf electric field of 250 kV/m and a dielectric loss of 100 W [4, p. 87]. The original window suffers from window failure while the raised window seldomly does. The dielectric losses are insufficient to account for the window failure and Rimmer conjectured [4, p. 107] that 500 W of heat deposited onto the window could be capable of causing either thermal or stress failure. It is tantalizing to observe that one per cent of the rf power, amounting to 400 W for Rimmer's experiments, may make up for the required heat of 500 W needed to cause either type of failure. Equally tantalizing is the suseptibility diagram constructed for Beryllia with $\delta_{\max 0} = 3.4$ and $E_{\max 0} = 2$ kV [4, p. 18]. This diagram (not shown, since it is quite similar to Fig. 4) yields a threshold rf electric field on the order of 200 kV/m, a value much closer to the raised window than to the original window. The present theory then seems to support Rimmer's speculations, quoted in the Introduction, on the possibly important role played by multipactor on window failure [17].

In our opinion, the weakest assumption is that the positive charge on the dielectric is uniformly distributed on the surface. This assumption leads to the simple form of (8). This drastic simplification should be kept in mind in view of the importance of the charging field to the saturation mechanism. Also neglected throughout is the possible gas desorption and ionization caused by electron bombardment of the saturated multipactor; these processes, important for dielectric breakdown under the dc condition [16], may well contribute to the last step of window failure.

ACKNOWLEDGMENT

The authors wish to thank R. Rimmer of Lawrence Berkeley Laboratory for making available to us his thesis [4]. They also wish to thank him and D. Chernin for many useful discussions.

REFERENCES

[1] J. R. M. Vaughan, "Multipactor," *IEEE Trans. Electron Devices*, vol. 35, p. 1172, 1988.
[2] D. H. Preist and R. C. Talcott, "On the heating of output windows of microwave tubes by electron bombardment," *IRE Trans. Electron Devices*, vol. ED-8, p. 243, 1961.
[3] J. R. M. Vaughan, "Some high-power window failures," *IEEE Trans. Electron Devices*, vol. ED-8, p. 302, 1961.
[4] R. A. Rimmer, "High power microwave window failures," Ph.D. dissertation, Univ. Lancaster, U.K., 1988.
[5] S. Yamaguchi, Y. Saito, S. Anami, and S. Michizono, "Trajectory simulation of multipactoring electrons in an S-band pillbox RF window," *IEEE Trans. Nucl. Sci.*, vol. 39, p. 278, 1992.
[6] N. Rozario *et al.*, "Investigation of Telstar 4 spacecraft Ku-band and C-band antenna components for multipactor breakdown," *IEEE Trans. Microwave Theory Tech.*, vol. 42, p. 558, 1994.
[7] R. A. Kishek, "Interaction of multipactor discharge with RF structures," Ph.D. dissertation, Univ. Michigan, Ann Arbor, 1997. See also [13]–[15].
[8] R. A. Kishek and Y. Y. Lau, "Multipactor discharge on a dielectric," *Phys. Rev. Lett.*, vol. 80, p. 193, 1998.
[9] While the "DC" electric field is allowed to evolve in time, we assume that it remains constant over the time of flight of a multipactoring electron. We shall use "DC field" and "charging field" interchangeably to denote the restoring electric field, E_{DC}, shown in Fig. 1.
[10] O. Hachenberg and W. Brauer, "Secondary electron emission from solids," *Advances in Electronics and Electron Physics XI*, L. Marton, Ed. New York: Academic, 1959, pp. 413–499.
[11] C. K. Birdsall and W. B. Bridges, *Electron Dynamics of Diode Regions*. New York: Academic, 1966.
[12] J. R. M. Vaughan, "A new formula for secondary emission yield," *IEEE Trans. Electron Devices*, vol. 36, p. 1963, 1989.
[13] R. Kishek and Y. Y. Lau, "Interaction of multipactor discharge and RF circuit," *Phys. Rev. Lett.*, vol. 75, p. 1218, 1995.
[14] ——— "A novel phase focusing mechanism in multipactor discharge," *Phys. Plasma*, vol. 3, p. 1481, 1996.
[15] R. A. Kishek, Y. Y. Lau, and D. Chernin, "Steady state multipactor and dependence on material properties," *Phys. Plasma*, vol. 4, p. 863, 1997, and references therein.
[16] R. A. Anderson and J. P. Brainard, "Mechanism of pulsed surface flashover involving electron-stimulated desorption," *J. Appl. Phys.*, vol. 51, p. 144, 1980.
[17] A. Neuber, J. Dickens, D. Hemmert, H. Krompholz, L. L. Hatfield, and M. Kristiansen, "Window breakdown caused by high power microwaves," this issue, pp. 296–303.

Lay-Kee Ang received the B.S. degree from National Tsinghua University, Hsinchu, Taiwan, R.O.C., in 1994, and the M.S. degree in 1996 from the University of Michigan, Ann Arbor, where he is currently pursuing the Ph.D. degree. His interests are in laser ablation of materials, multipactor discharge, and high power microwave source. He has several publications on these subjects.

Y. Y. Lau, for a photograph and biography, see this issue, p. 234.

Rami A. Kishek was born in Palestine in March 1973. He received the B.S.E. degree in electrical engineering in 1993, the M.S.E. degree in nuclear engineering in 1995, and the Ph.D. degree, also in nuclear engineering, in 1997, all from the University of Michigan, Ann Arbor, where he did his graduate work on multipactor discharge.

He has since been working as a post-doctorate at the Institute for Plasma Research, University of Maryland, College Park, in the area space-charge-dominated beam dynamics and beam transport for the Maryland Electron Ring. His research interests revolve on rf discharges and microwave generation, as well as on beam physics and PIC code simulations. He has written a review article on multipactor discharge.

Ronald M. Gilgenbach (S'73–M'74–SM'92), for a photograph and biography, see this issue, p. 288.